Applying multi-scale silica-like three-dimensional networks in PEO matrix via in-situ crosslinking for high-performance solid composite electrolyte

Jiawei Wu [1], Jing Chen [1], Xiaodong Wang [2], An'an Zhou [3], Zhenglong Yang *, [1]

[1]Key Laboratory of Advanced Civil Engineering Materials of Ministry of Education, School of Materials Science and Engineering, Tongji University, Shanghai 200092, P. R. China;

[2]Shanghai Key Laboratory of Special Artificial Microstructure Materials and Technology & School of Physics Science and Engineering, Tongji University, Shanghai 200092, P. R. China;

[3]School of Biological & Chemical Engineering, Zhejiang University of Science & Technology, Hangzhou 310023, P. R. China.

** Corresponding author.*

E-mail: yangzhenglong@tongji.edu.cn; Tel: +86-21-69584723

Calculation of crystallinity rate

The corresponding crystallinity(χ_c) of the SPE was calculated according to the following equation:

$$\chi_c = \frac{S_{m-peak}}{S_{m-peak}^{pure\ PEO} f_{PEO}} \times 100\%$$

Where $S_{m\text{-}peak}$ is the integral area of melting peak of different samples in the DSC curve, f_{PEO} is the mass percentage of PEO in different samples.

Fitting of the Vogel-Tamman-Fulcher (VTF) quasi-thermodynamic model

The conductivity-temperature curves of different samples were fitted to VTF conducting model via the following equation:

$$\sigma = AT^{-1/2} e^{\frac{-E_a}{T-T_0}}$$

Where A is the former factor, which relates to the concentration of carriers in theory, E_a is the activation energy, T_0 is thermodynamic equilibrium temperature for ideal glass transition.

Calculation of the distribution of the nano SiO_2 samples

Series of distribution curves in the aspect of diameter and length were calculated by classifying the products (over 150 times per sample) into different classes (discrete but uniform) via observing the SEM images of different samples (such as **Fig. 1(a)-(d)** in the manuscript). Secondly, an orthogonal multiply was conducted to acquire 2D distribution cloud maps of different samples, which realizes the combination of length and diameter.

In this work, the ratio of length to diameter was set as the standard: ≤2 was taken as sphere (particle), with ≤10 taken as rod and >10 taken as wire. In this way, the 2D maps were divided into several regions (the slope of the top cut-off straight is 10, the second is 2 and the last is 1 in **Fig. S3**). By summing up the relative frequencies of different regions and making calibrations, the proportions of the three kinds could be calculated.

Table S1 Detailed components of each sample

Sample	PEO/ g	EO_1/ mol	LiTFSI /g	SiO_2/ g	PEA- GPS/ g	EO_2/ mol	G-mPEG /g	EO_3/ mol	ΣEO/ mol	Σm_{GPS}/ g	Σm/ g
PEO-SNW	0.160	0.00364	0.058	0.018					0.00364		0.23600
PEO-SNWAKP60	0.103	0.00235	0.058	0.018	0.0731	0.00081	0.0388	0.00048	0.00364	0.0391	0.29136
PEO-SNWAKP40	0.105	0.00238	0.058	0.018	0.0487	0.00054	0.0582	0.00072	0.00364	0.0391	0.28775
PEO-SNWAKP30	0.106	0.00240	0.058	0.018	0.0365	0.00041	0.0679	0.00084	0.00364	0.0391	0.28595
PEO-SNWAKP20	0.106	0.00241	0.058	0.018	0.0243	0.00027	0.0776	0.00096	0.00364	0.0391	0.28415
PEO-SNWAKP10	0.107	0.00243	0.058	0.018	0.0122	0.00014	0.0873	0.00108	0.00364	0.0391	0.28235

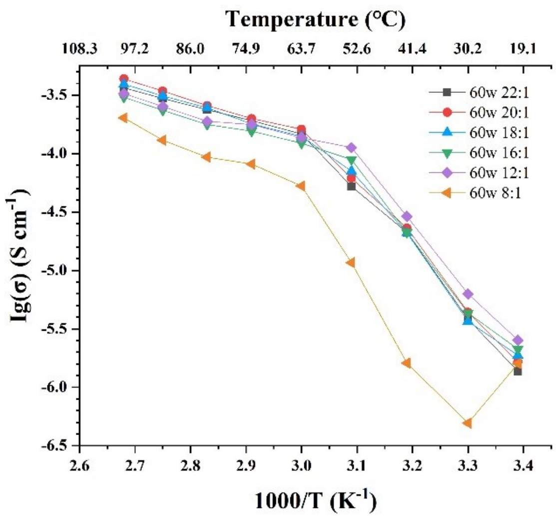

Figure S1 Conductivity-temperature curves of PEO matrix with a different amount of LITFSI

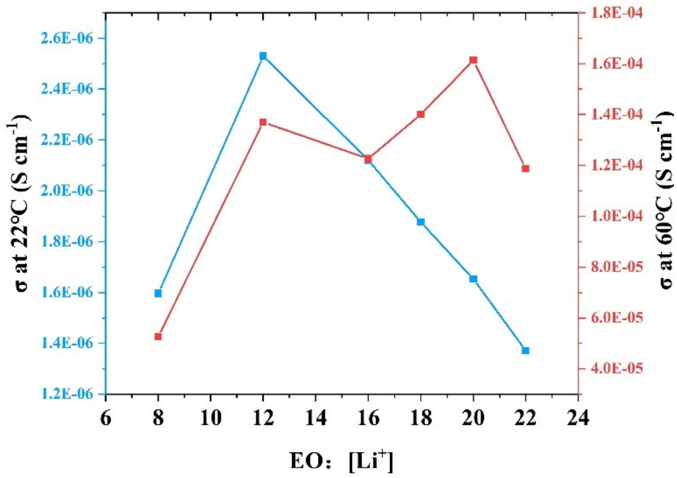

Figure S2 Conductivity of PEO matrix with different amounts of LITFSI at 22 and 60 ^{o}C, respectively

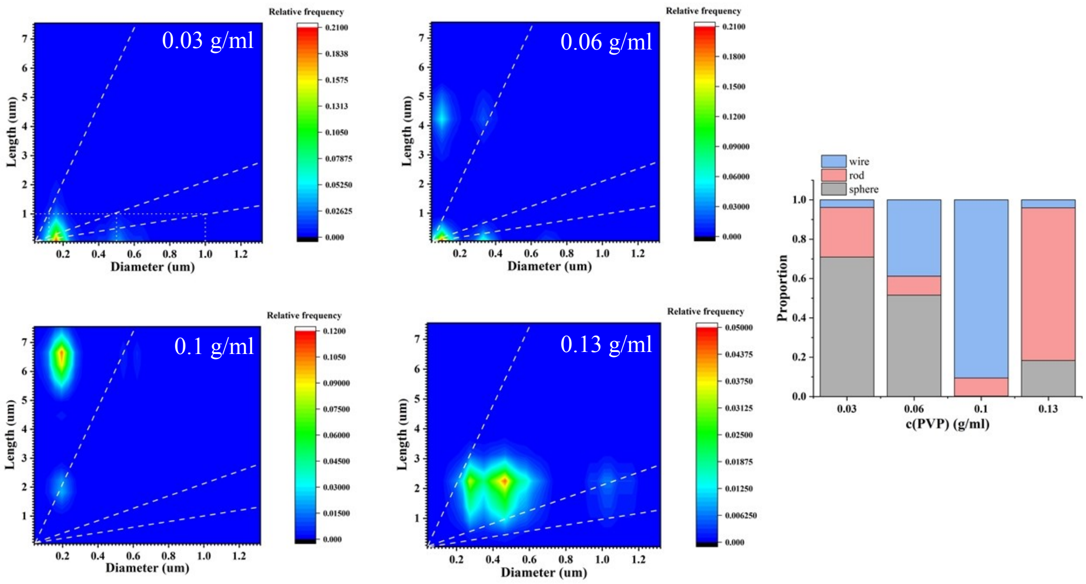

Figure S3 The influence of the concentration of PVP on the morphology of SiO_2. The tag in the upper-right corner was the concentration of PVP. (the concentration of sodium citrate solution was fixed as 0.18 M and that of TEOS was fixed a 1:75).

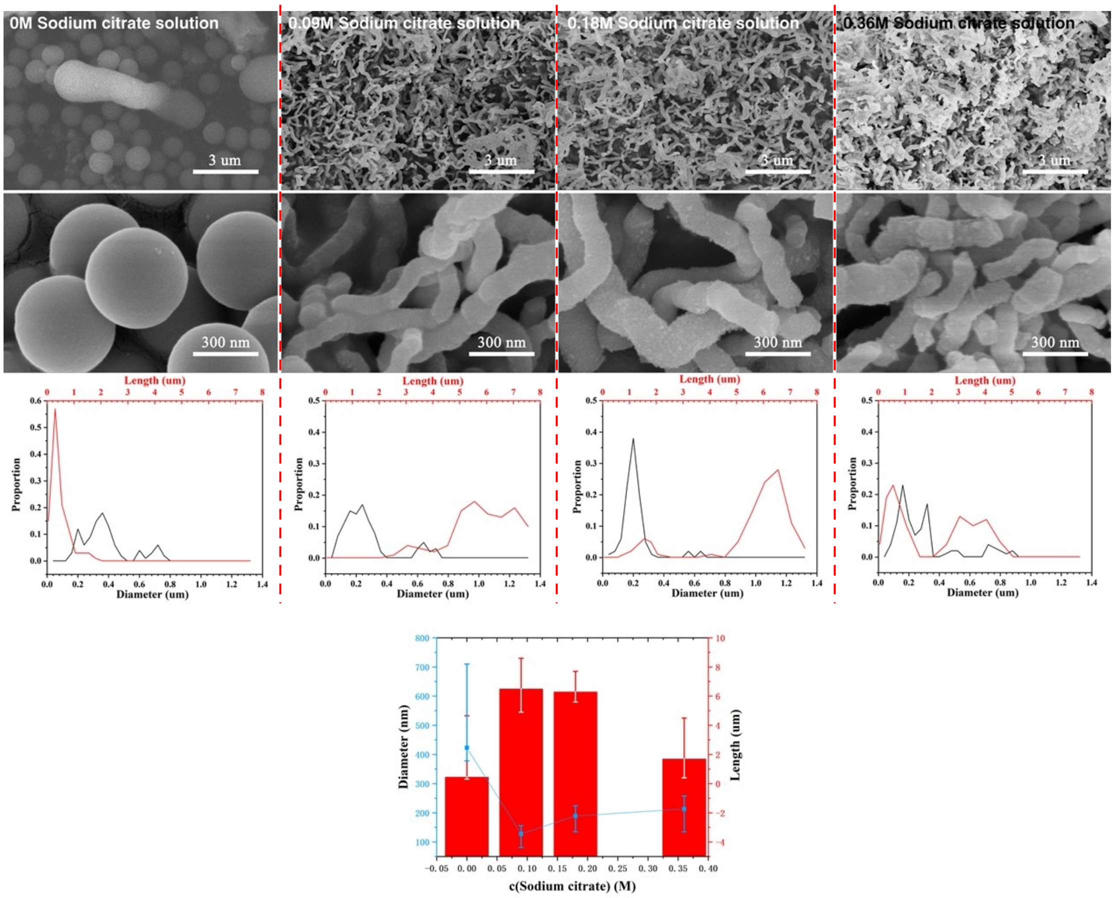

Figure S4 The influence of the concentration of sodium citrate solution on the morphology of SiO_2. The tag in the upper left corner was the concentration of sodium citrate solution. (the concentration of PVP was fixed as 0.1 g/ml and that of TEOS was fixed a 1:75)

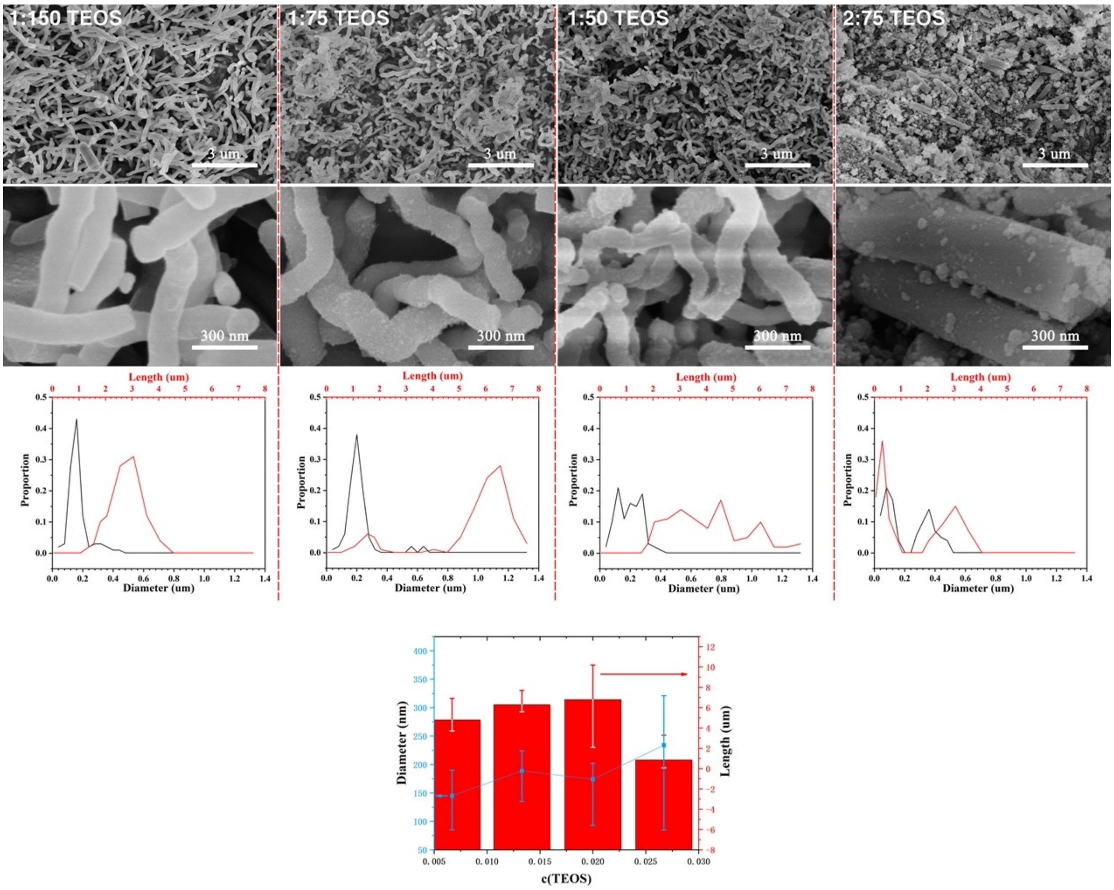

Figure S5 The influence of the concentration of sodium citrate solution on the morphology of SiO_2. The ratio in the upper left corner was the volume of TEOS to ethanol. (the concentration of sodium citrate solution was fixed as 0.18 M and that of PVP was fixed as 0.1 g/ml)

.

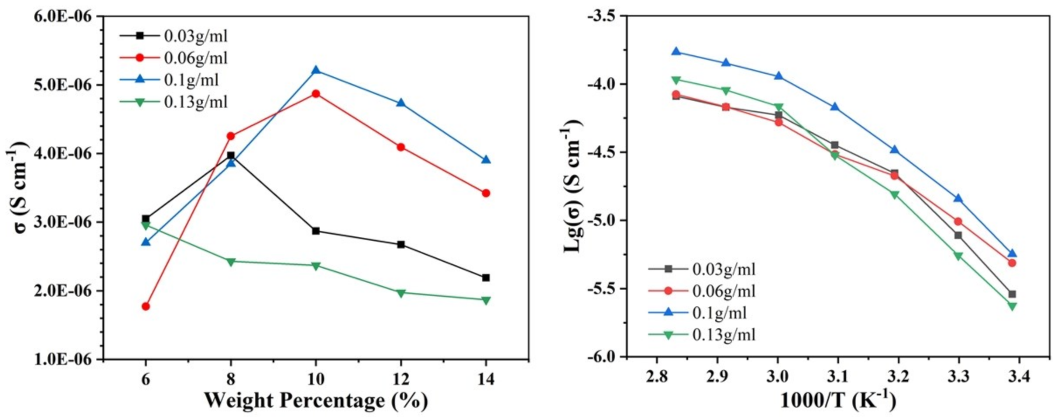

Figure S6 The ionic conductivity of PEO-SNW with various amounts of nano SiO_2 fabricated under different concentration of PVP at 22 ^{o}C and the temperature-conductivity curves of PEO-SNW with 10 wt.% nano SiO_2 fabricated under different concentration of PVP

Table S2 VTF fitting result of different PEO-SNW

Sample	A/S❿K$^{1/2}$❿cm^{-1}	E_a/K	E_a/J❿mol^{-1}	T_0/K	R^2(COD)	R^2_{modify}
PEO-SNW(0.03g/ml PVP)	0.0089	297.1	2470	267.1	0.9964	0.9946
PEO-SNW(0.06g/ml PVP)	0.0226	445.2	3701	243.7	0.9977	0.9965
PEO-SNW(0.1g/ml PVP)	0.0432	388.7	3232	254.7	0.9971	0.9957
PEO-SNW(0.13g/ml PVP)	0.0999	493.7	4105	241.9	0.9939	0.9909

Table S3 VTF fitting result of different samples

Sample	A/S❿K$^{1/2}$❿cm^{-1}	E_a/K	E_a/J❿mol^{-1}	T_0/K	R^2(COD)	R^2_{modify}
PEO	0.1662	345.8	2875	255.9	0.9824	0.9765
PEO-SNW	0.7563	451.0	3750	248.1	0.9790	0.9721
PEO-SNWAKP60	0.3227	417.9	3474	253.5	0.9625	0.9536
PEO-SNWAKP40	0.2248	250.5	2083	262.6	0.9888	0.9851
PEO-SNWAKP30	0.0623	118.6	986.1	274.9	0.9890	0.9853
PEO-SNWAKP20	0.1280	142.7	1187	271.3	0.9942	0.9922
PEO-SNWAKP10	0.1633	173.3	1441	268.7	0.9962	0.9950

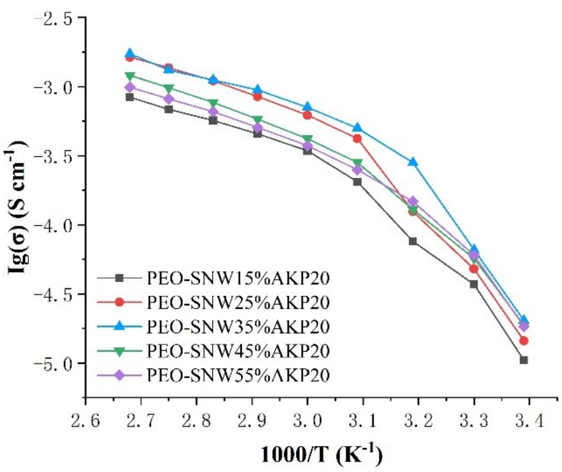

Figure S7 The conductivity-temperture curves of samples with different amounts of AKP20. This ratio was set as 35 % in the manuscript, corresponding to the percentage of EO from AKP.

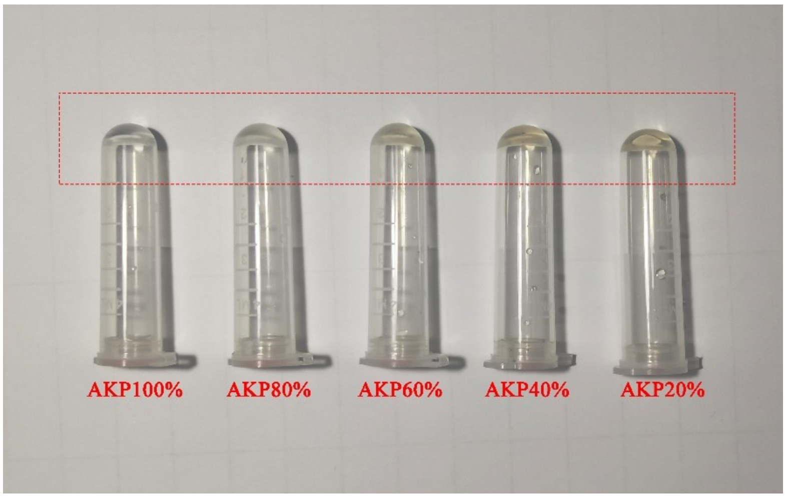

Figure S8 Bulk formed by AKP with different percentages of PEA-GPS. The percentage followed is the addition amount of PEA -GPS.

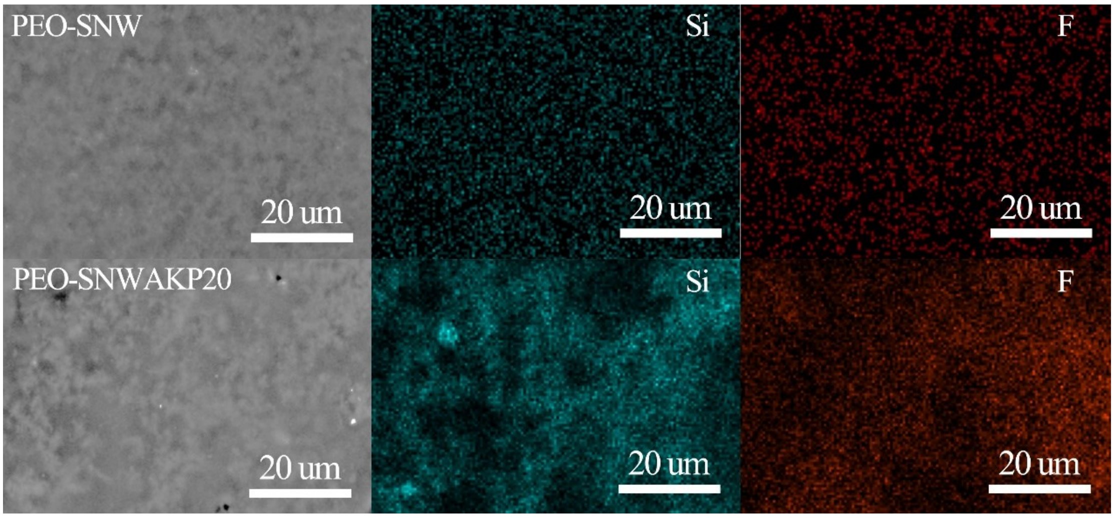

Figure S9 SEM image of the surface of PEO-SNW, PEO-SNWAKP and the followings are Si, F mapping of the corresponding area.

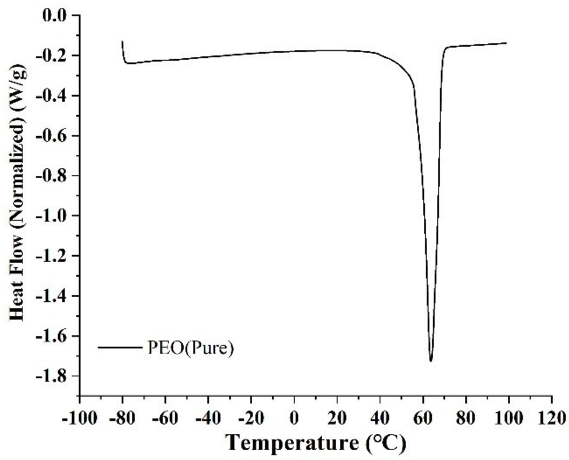

Figure S10 DSC curve of pure PEO without adding LITFSI

Table S4 Calculation result of different samples

Sample	T_g/℃	T_m/℃	$S_{m\text{-}peak}$	m_{PEO}/%	χ_c/%
PEO(Pure)		64.2	12.3415	1	100
PEO	-47.2	51.2	4.45768	73.40	49.12
PEO-SNW	-48.5	50.7	4.02351	67.80	48.08
PEO-SNWAKP60	-58.8	32.4	1.51702	35.35	34.77
PEO-SNWAKP40	-64.2	41.2	2.71931	36.49	60.38
PEO-SNWAKP30	-64.7	40.6	2.58648	37.07	56.53
PEO-SNWAKP20	-64.6	40.5	2.39113	37.30	51.94
PEO-SNWAKP10	-49.4	39.8	2.06144	37.90	44.07

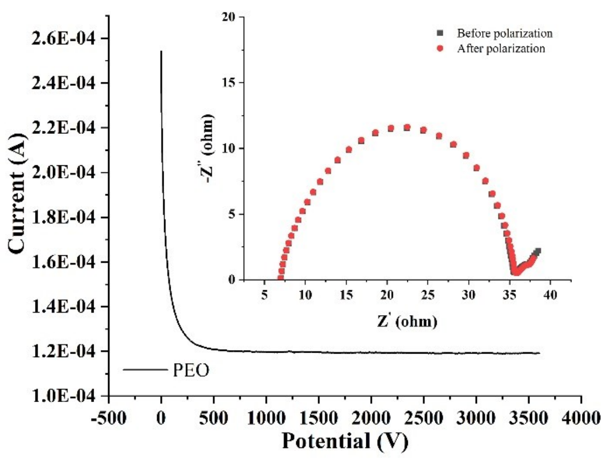

Figure S11 i-t and corresponding IMP curves of blank PEO sample at 70 ^{o}C

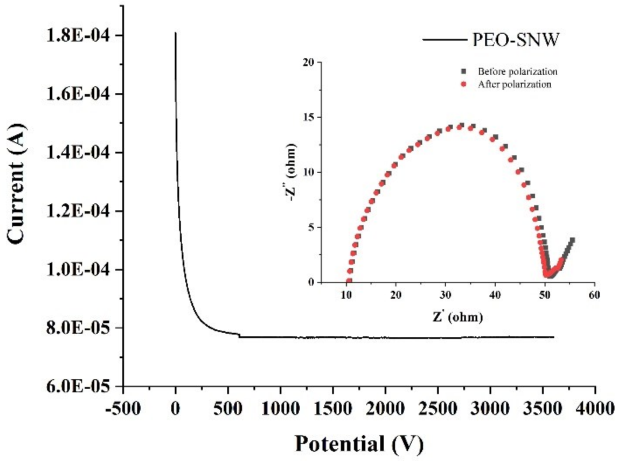

Figure S12 i-t and corresponding IMP curves of PEO-SNW at 70 ^{o}C

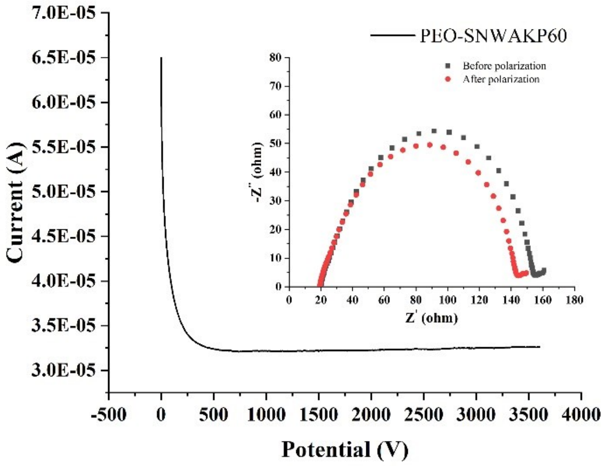

Figure S13 i-t and corresponding IMP curves of PEO-SNWAKP60 at 70 ^{o}C

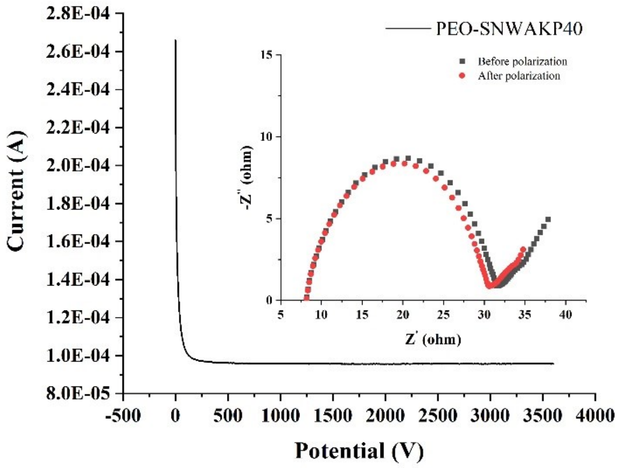

Figure S14 i-t and corresponding IMP curves of PEO-SNWAKP40 at 70 ^{o}C

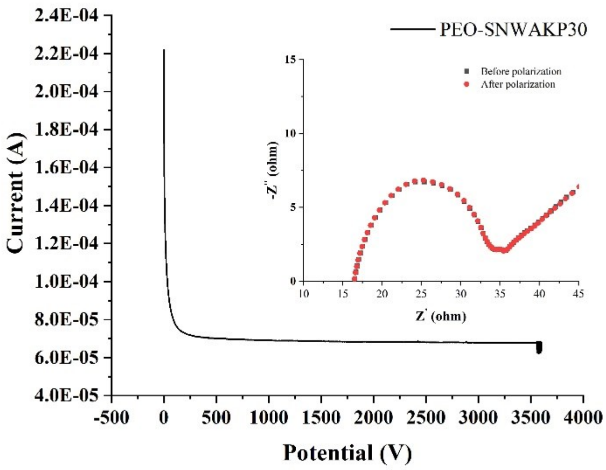

Figure S15 i-t and corresponding IMP curves of PEO-SNWAKP30 at 70 ^{o}C

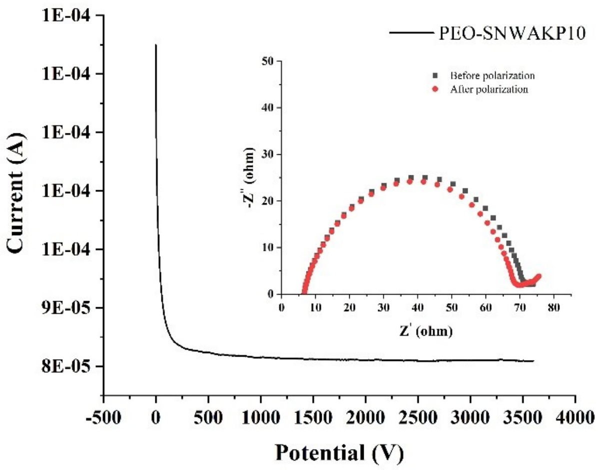

Figure S16 i-t and corresponding IMP curves of PEO-SNWAKP10 at 70 ^{o}C

Table S5 t^{+} of the representatives of different samples

Sample	V/V	I_0/A	I_s/A	R_b^0/Ω	R_b^s/Ω	R_i^0/Ω	R_i^s/Ω	t^{+}
PEO	0.01	2.54E-4	1.19E-4	7.188	7.139	28.45	28.65	0.1985
PEO-SNW	0.01	1.81E-4	7.69E-5	10.8	10.56	40.38	37.79	0.1648
PEO-SNWAKP60	0.01	6.50E-5	3.26E-5	19.66	19.05	127.2	122	0.1487
PEO-SNWAKP40	0.01	2.66E-4	9.57E-5	8.298	8.278	22.96	22	0.1778
PEO-SNWAKP30	0.01	2.22E-4	6.78E-5	16.44	16.59	18.24	17.69	0.2046
PEO-SNWAKP10	0.01	1.35E-4	8.09E-5	6.678	6.805	64.56	62.29	0.1553